The Design and Testing of RoboClam: A Machine Used to Investigate and Optimize Razor Clam-Inspired Burrowing Mechanisms for Engineering Applications

Proceedings of the ASME 2009 International Design Engineering Technical Conferences & Computers and Information in Engineering Conference
IDETC/CIE 2009
August 30 - September 2, 2009, San Diego, California, USA

DETC2009-86808

THE DESIGN AND TESTING OF ROBOCLAM: A MACHINE USED TO INVESTIGATE AND OPTIMIZE RAZOR CLAM-INSPIRED BURROWING MECHANISMS FOR ENGINEERING APPLICATIONS

Amos G. Winter, V
Hatsopolous Microfluids Laboratory
Precision Engineering Research Group

A.E. Hosoi*
Hatsopolous Microfluids Laboratory

Alexander H. Slocum
Precision Engineering Research Group

Robin L.H. Deits
Hatsopolous Microfluids Laboratory

Department of Mechanical Engineering
Massachusetts Institute of Technology, Cambridge, Massachusetts 02139, U.S.A.

ABSTRACT

Razor clams (*Ensis directus*) are one of nature's most adept burrowing organisms, able to dig to 70cm at nearly 1cm/s using only 0.21J/cm. *Ensis* reduces burrowing drag by using motions of its shell to fluidize a thin layer of substrate around its body. Although these shell motions have an energetic cost, moving through fluidized rather than packed soil results in exponentially lower overall energy consumption. This paper describes the design and testing of RoboClam, a device that mimics *Ensis* digging methods to understand the limits of razor clam-inspired burrowing, how they scale for different environments and conditions, and how they can be transferred into engineering applications. Using a genetic optimization solver, we found that RoboClam's most efficient digging motion mimicked *Ensis* shell kinematics and yielded a power law relationship between digging energy and depth of $n = 1.17$, very close to the ideal value of $n = 1$. Pushing through static soil has a theoretical energy-depth power law of $n = 2$, which means that *Ensis*-inspired burrowing motions can provide exponentially higher energy efficiency and nearly depth-independent drag resistance.

1 INTRODUCTION

The motivation behind our work is to generate compact, lightweight, low-energy, reversible, and dynamic burrowing and anchoring systems for use in subsea applications. As many organisms have evolved to embed themselves into undersea substrates [1-11], our hypothesis is that nature has found an optimized solution to subsea burrowing. This paper describes the design and testing of RoboClam, a robot that mimics the kinematics of the Atlantic razor clam, *Ensis directus*, in order to probe the limits of *Ensis*-inspired burrowing.

We identified *Ensis* as the best candidate for biomimicry because of its performance and engineering merits [2, 10, 11]. *Ensis* burrows at nearly 1cm/s to 70cm deep using approximately 0.21J/cm, which equates to being able to travel over a half kilometer on the energy in a AA battery [12]. Furthermore, razor clams are the size scale of a real engineering device (3.2cm diameter, 16cm long), and are packaged in a rigid shell with only one degree-of-freedom movement. Using this performance and the animal's geometry, we have calculated that an *Ensis*-based burrowing/anchoring system would provide a 10X improvement over the best currently available anchoring technology, leading most by more than two orders of magnitude, in anchoring force developed per unit energy expended [13-15].

The burrowing cycle of a razor clam is shown in Fig. 1a. The animal starts with its foot - a soft, flexible organ - fully extended below the shell. Next, it uses a series of four shell motions to make downward progress: 1) the foot extends to uplift the shell; 2) the shell halves contract to force blood into the foot, inflating it to serve as an anchor; 3) the foot muscles contract to pull the shell downwards; and 4) the shell expands in order to begin the cycle again. To understand the soil mechanics during this cycle, we developed an experimental setup to visualize a razor clam burring in 1mm soda lime glass

* Associate Professor and author of correspondence, Phone: (617) 253-4337, Email: peko@mit.edu

beads, which are similar in size and density to course sand [16]. A video of *Ensis* burrowing in our setup can be seen here [17]. Substrate deformation was tracked using particle image velocimetry (PIV) [18]. We discovered that the uplift and contraction movements of the shell draw water towards the animal's body, unpacking and fluidizing the surrounding substrate, as shown in Fig. 1c.

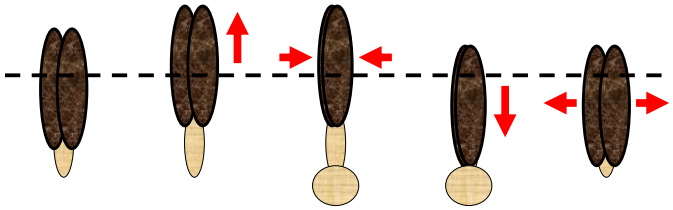

a. *Ensis* burrowing cycle

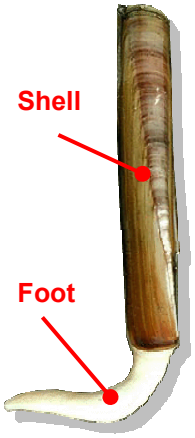

b. *Ensis* functional components

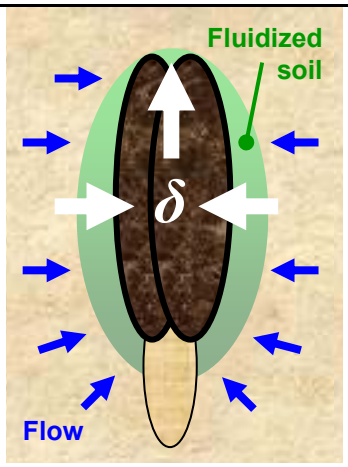

c. Localized fluidization of soil from uplift and contraction of shell

Figure 1. *Ensis* burrowing mechanics

Moving through a fluidized, rather than a packed, static substrate, results in drastic drag and energy reductions for the razor clam [19]. Figure 2 shows energy expended vs. depth for *Ensis* compared to a blunt body the same size and shape. *Ensis* data was interpolated from historical results [9], and blunt body data was measured in razor clam habitat off Gloucester, Massachusetts. The power law relationship of n = 2 for the blunt body is expected [20], as the soil strength should increase with depth. Although there is an energetic cost for the uplift and contraction movements, *Ensis* is able to achieve drastic energy savings and a power law relationship of n = 1, which indicates that drag on the clam is independent of depth.

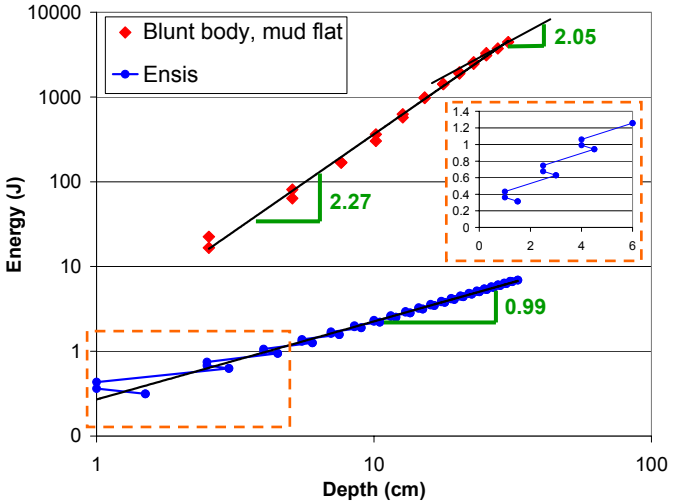

Figure 2. *Ensis* vs. blunt body energy expenditure

2 ROBOCLAM DESIGN

RoboClam was designed to replicate the digging kinematics of *Ensis* in order to verify that localized fluidization drag reduction could be transferred to engineering burrowing applications. Furthermore, RoboClam was designed to yield insight into the relationships between environmental and engineering parameters, such as substrate type, depth, device size, burrowing velocity, and required power.

2.1 DEVICE SCALING

A razor clam outputs a peak power of approximately 1.0W during its downward stroke [9], which is dissipated in the surrounding substrate. If the fluidized substrate is responsible for drag, the power required to submerge would scale with size squared and velocity cubed. This assumes high Reynolds number flow - the worst case scenario compared to power dissipated in Stoke's flow, which scales linearly with size and with the square of velocity [21].

A requirement of RoboClam was that it could be tested in real marine substrates, as to avoid wall effects caused by a container, and to capture the peculiarities of real soil with heterogeneous composition and the presence of organic matter. To do this, RoboClam required a power source compatible with marine environments. A standard 80 ft^3 scuba tank was a logical choice, as it contains about one-quarter the energy of a 12V 35Ah lead acid car battery [22, 23]. The scuba tank enabled our robotic "clam" to be sized from 0.5X to 2X *Ensis*, move up to 3X as fast, and run for nearly 1.5h at max size and velocity.

2.2 CLAM MECHANISM DESIGN AND ANALYSIS

RoboClam uses an *Ensis*-shaped end effector to dig into soil. The end effector required two degree-of-freedom motion: up/down and in/out. *Ensis* opens and closes its shell approximately 6.4mm (0.25in). To test the effect of in/out displacement on burrowing, the end effector was designed to

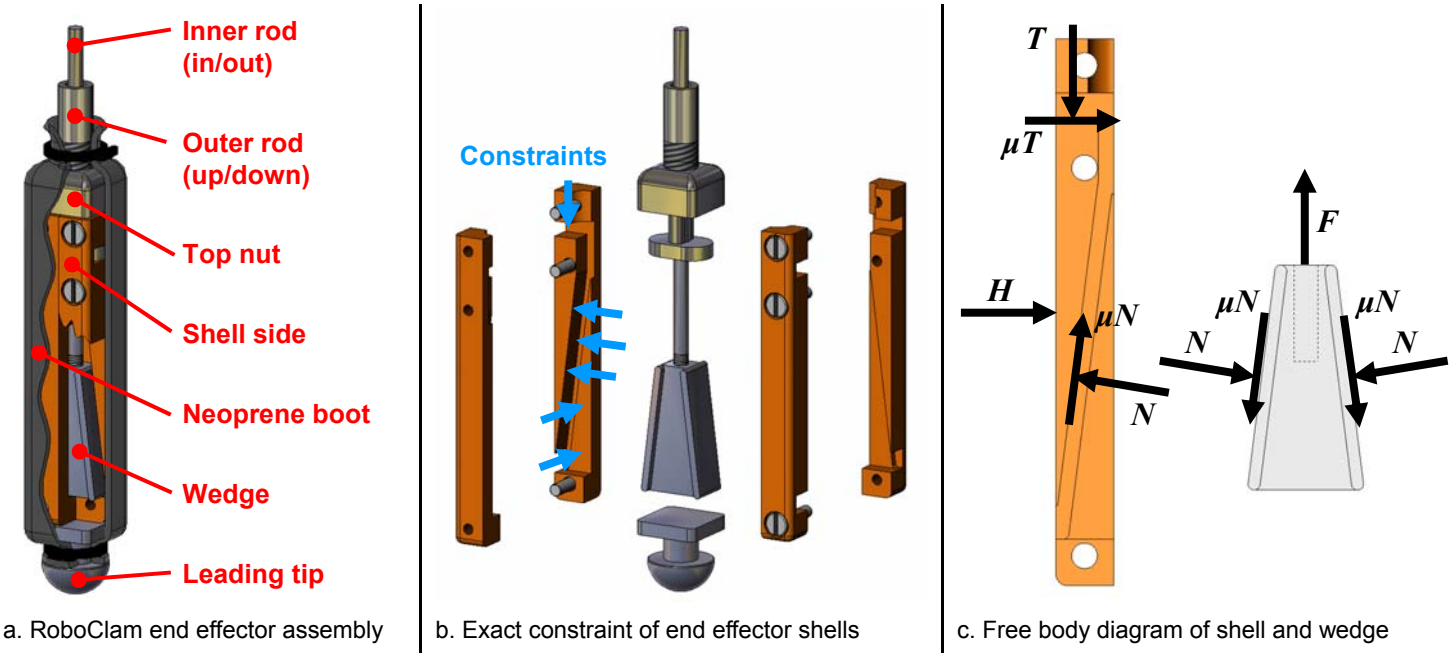

a. RoboClam end effector assembly b. Exact constraint of end effector shells c. Free body diagram of shell and wedge

Figure 3. RoboClam end effector design

open 2X as far as *Ensis*. This required the 0.5X scale end effector, which is only 9.97cm long and 1.52cm wide, to open 6.4mm. We accomplished this with a sliding wedge between the two "shells" of the end effector, as shown in Fig. 3. This mechanism is exactly constrained and has contact lengths/widths greater than two, as to prohibit jamming during any part of the stroke [24]. Furthermore, the wedge intersects the center of pressure on the shell regardless of its position. This prevents the shell from exerting moments on the wedge that could increase frictional losses. The rod used to actuate in/out movement is housed within the rod to move the end effector up and down, providing a compact coupling to RoboClam's actuation and measurement systems. The effector is surrounded by a neoprene boot to prevent soil particles from entering the mechanism.

The transmission ratio (*TR*) for the mechanism, given in Eq. 1, can be derived from the free body diagram in Fig. 3c.

$$TR = \frac{H}{F} = \frac{1}{2}\left[\frac{\cos\theta - \mu\sin\theta}{\sin\theta + \mu\cos\theta} - \mu\right] \quad (1)$$

The efficiency of the mechanism, given in equation 2, can be calculated by computing the work done over a stroke.

$$\eta = \frac{E_{in}}{E_{out}} = 2\frac{H\delta_x}{F\delta_y} = 2TR\sin\theta \quad (2)$$

The end effector is made from alloy 932 (SAE 660) bearing bronze and 440C stainless steel. These materials were chosen because both are saltwater compatible and have a low coefficient of sliding friction when lubricated [25]. The dynamic coefficient of friction within the mechanism was measured to be 0.173 with 0.013 standard deviation under horizontal loads ranging from 13.34N to 83.74N. Silicon oil was used as a lubricant because it does not get absorbed by the neoprene boot.

The wedge angle was chosen to be 7.13° in order to maximize contact lengths/widths while enabling the mechanism to be as small as a 0.5X scale *Ensis*. Since the *TR* increases with decreased θ and μ, this geometry yields a relatively high *TR* of 1.55, with a maximum of 1.83 and minimum of 1.33 corresponding to 6σ friction measurements. The corresponding efficiency is 39% with a minimum of 33% and a maximum of 46%. This level of efficiency is tolerable; packaging size, jam-free operation, and the ability to deterministically calculate lost energy outweigh the need for high efficiency. If efficiency is critical in future design iterations, a maximum of 60% can be achieved using a similar wedge design with the same materials and a wedge angle of 29°.

2.3 ROBOT PACKAGING

The RoboClam actuation system is composed of two nested pneumatic pistons, as shown in Fig. 4. The lower piston rod connects to the top of the end effector and controls up/down movement, serving the same roll as the foot on *Ensis*. The upper cylinder controls the in/out motion of the effector mechanism via a connecting rod that runs through the center of the lower piston rod. The nested piston configuration was chosen because it enables each degree of freedom to be actuated independently and provides a low-profile connection to the end effector.

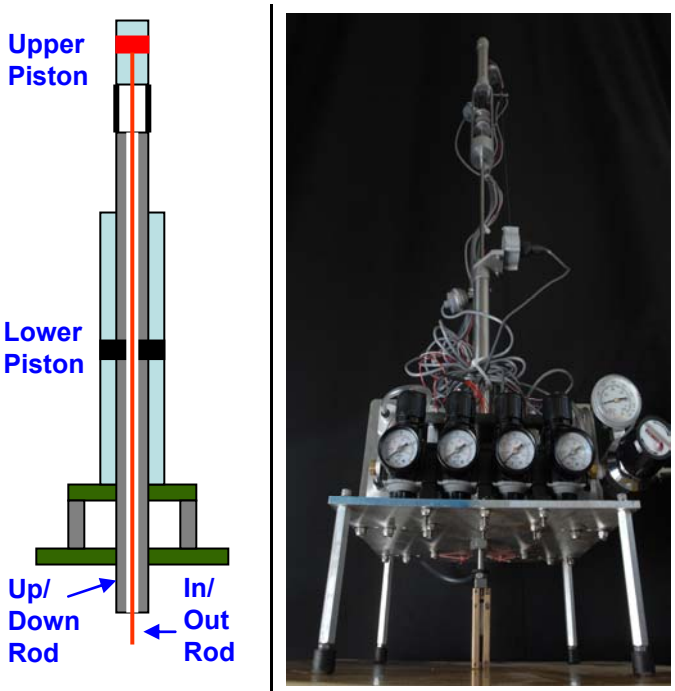

a. Piston schematic b. Full RoboClam [26]

Figure 4. RoboClam actuation system and packaging layout

Pressure is regulated down from the scuba tank to four independent regulators, one for each piston inlet. Air pressure delivered to the pistons is measured by a transducer at each input port. Displacements of the lower and upper pistons are measured by a string potentiometer and an integrated linear potentiometer, respectively. Sensor excitation, data acquisition, and control of the solenoid valves that send air to the pistons are managed by a USB DAQ device run through LabView [27]. Power to the DAQ is provided by USB, and power to the solenoid valves is provided by two small onboard lead acid batteries.

2.4 ENERGY EXPENDITURE CALIBRATION

To determine whether *Ensis*-inspired digging provides and advantage over other methods, the energy expended in soil deformation while burrowing must be calculated. The overall energy consumed is device dependent; we are interested in finding a new burrowing *method* that is more efficient than current methods. After this method is identified, machines used to exploit it can be designed for optimized efficiency.

Soil deformation energy can be calculated by accounting for input energy minus all of the other losses in the system. For the up/down motion of RoboClam, the energy lost to soil deformation during one stroke is

$$\begin{aligned} E_{soil} &= E_{in} - E_{friction} - E_{potential} \\ &= \int_{\delta_1}^{\delta_2} \Delta p_u A_u dy - \left| F_{u,friction}(\delta_2 - \delta_1) \right| \\ &\quad - m_u g(\delta_2 - \delta_1) \end{aligned} \tag{3}$$

where the subscript u designates the up/down piston, Δp_u is the pressure difference over the piston, δ_1 and δ_2 are the starting and ending displacements of the stroke, A_u is the area of the piston, $F_{u,friction}$ is the measured frictional force in the piston, and m_u is the total mass moving up and down.

The energy transferred to the soil during the in/out motion is represented by

$$\begin{aligned} E_{soil} &= \eta(E_{in} - E_{friction} - E_{potential}) - E_{boot} \\ &= \eta\left[\int_{\delta_1}^{\delta_2} \Delta p_i A_i dy - \left| F_{i,friction}(\delta_2 - \delta_1) \right| \right. \\ &\quad \left. - m_i g(\delta_2 - \delta_1)\right] \end{aligned} \tag{4}$$

where the subscript i represents the in/out piston, δ_1 and δ_2 are the starting and ending displacements of the stroke, η is the efficiency defined in Equation 2, Δp_i is the pressure difference over the piston, A_i is the area of the piston, $F_{i,friction}$ is the measured frictional force in the piston, and m_i is the total mass moving up and down. E_{boot} proved to be very difficult to measure. Since this energy results from elastic deflection of boot, it was taken to be zero over a full in/out cycle. This is a conservative assumption, as any energy lost to hysteresis caused by the viscoelasticity of the neoprene will appear as additional energy dissipated in the soil.

3 EXPERIMENTAL METHOD

RoboClam was tested in a substrate composed of 1mm soda lime glass beads, the same substrate used in our *Ensis* visualization system. Three different kinematic motions were trialed in order to form energetic comparisons between burrowing methods: 1) pushing straight down; 2) opening the effector in and out and letting it fall under gravity; and 3) mimicking the up/in/down/out clam motion. The minimum energy required to push straight down was found by measuring the minimum pressure required to fully submerge the end effector. The minimum energy required for the in/out-only method was determined by minimizing the pressure required to open and close the effector at full depth. In this test the end effector was opened and closed the full 6.4mm stroke.

The minimum energy required to dig using the full up/in/down/out clam motion was optimized using MATLAB's Genetic Algorithm Solver [28]. This program approximates the evolution of a biological system by generating a population of parameters, in our case the upward stroke time and the downward stroke distance, and then selecting the sets of

parameters that display the best minimum 'fitness'. The fitness value was taken to be the product of the energy expended per unit depth and the exponent of the energy vs. depth power law relationship. This product was chosen as the fitness value since optimizing one of the parameters alone resulted in highly undesirable values of the other.

4 RESULTS AND DISCUSSION

Figure 5a shows the optimized soil deformation energy vs. depth for the three digging methods. These plots were calculated using equations 4 and 5 with the appropriate friction and mass values. As expected, the clam-inspired up/in/down/out motion requires the least amount of total energy over RoboClam's full vertical deflection. The times and displacements of this motion, generated by the Genetic Algorithm, are: 0.032s up, 6.5mm in, 5cm down, and 6.5mm out. The mean coefficient of friction in the end effector mechanism was used to generate the curves; applying 6σ friction variation does not change the overall result.

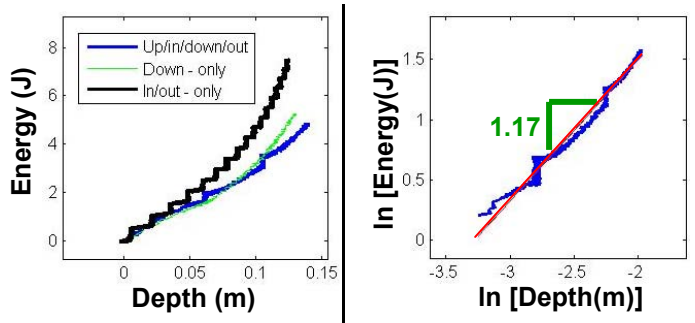

a. Energy expended to soil for different burrowing methods

b. Power law relationship for up/in/down/out burrowing

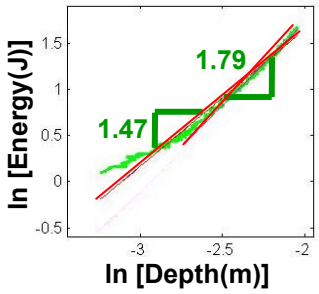

c. Power law relationship for pushing straight down

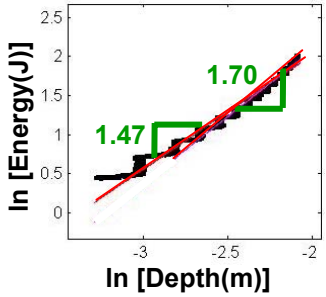

d. Power law relationship for in/out-only burrowing

Figure 5. Energy vs. depth for different burrowing motions

Figures 5b-d show the power law relationship for each method of digging. The up/in/down/out motion shown in Fig. 5b yields a significantly lower slope compared to the other two methods, close to the expected value of $n = 1$. Accounting for 6σ variability in friction within the effector yields a minimum of $n = 1.16$ and a maximum of $n = 1.19$. The slope for pushing straight down, shown in Fig. 5c, was measured to be $n = 1.47$, increasing to $n = 1.79$ over the last 5cm. This is very close to the expected value of $n = 2$. The change in slope may be due to soil surface effects, as RoboClam's displacement was limited to 14cm. Figure 5d illustrates that the in/out-only motion provides no energetic benefits, with the slope increasing to $n = 1.70$ over the last 5cm.

5 CONCLUDING REMARKS AND FUTURE WORK

Three exciting conclusions can be drawn from the presented RoboClam test data. First, RoboClam successfully replicated the kinematics of a burrowing *Ensis* and achieved similar drag reduction. Second, *Ensis*-inspired digging provides exponentially better energy efficiency compared to simply pushing a blunt body through soil. Third, the *Ensis*-like motion results in energy savings in spite of the cost of moving upwards, contracting in, and expanding out – motions that do not directly contribute to downward progress.

We are currently developing the 1X and 2X size scale end effectors for RoboClam. We will use these devices to further understand the limits of *Ensis*-inspired digging by testing RoboClam in different substrates, depths, and kinematic configurations. Concurrently with experimentation, we are developing theoretical soil/fluid constitutive models to describe the fluidized region of substrate around a contracting body, as well as the drag associated with moving through the substrate. Empirical and theoretical results will be combined to form design rules to describe how to deterministically design a burrowing device for any size scale, substrate type, and performance requirements.

ACKNOWLEDGMENTS

This work was sponsored by the Battelle Memorial Institute of Columbus, OH, Bluefin Robotics of Cambridge, MA, and Chevron of Houston, TX.

REFERENCES

1. Fager, E.W., 1964, *Marine Sediments: Effects of a Tube-Building Polychaete,* Science, **143**(3604): p. 356-359.
2. Holland, A.F. and J.M. Dean, 1977, *Biology of Stout Razor Clam Tagelus-Plebeius .1. Animal-Sediment Relationships, Feeding Mechanism, and Community Biology.* Chesapeake Science, **18**(1): p. 58-66.
3. Aoyama, J., et al., 2005, *First observations of the burrows of Anguilla japonica.* Journal of Fish Biology, **67**(6): p. 1534-1543.
4. Kelly, M.D., et al., 2005, *Burrow extension by crack propagation,* Nature, **433**(7025): p. 475.
5. Rosenberg, R. and K. Ringdahl, 2005, *Quantification of biogenic 3-D structures in marine sediments.* Journal of Experimental Marine Biology and Ecology, **326**(1): p. 67-76.
6. Shin, P.K.S., A.W.M. Ng, and R.Y.H. Cheung, 2002, *Burrowing responses of the short-neck clam Ruditapes philippinarum to sediment contaminants.* Marine Pollution Bulletin, **45**(1-12): p. 133-139.

7. Stanley, S.M., 1969, *Bivalve Mollusk Burrowing Aided by Discordant Shell Ornamentation.* Science, **166**(3905): p. 634-635.
8. Trueman, E.R., 1966, *Bivalve Mollusks: Fluid Dynamics of Burrowing.* Science, **152**(3721): p. 523-525.
9. Trueman, E.R., 1967, *The Dynamics of Burrowing in Ensis (Bivalvia).* Proceedings of the Royal Society of London. Series B, Biological Sciences, **166**(1005): p. 459-476.
10. Trueman, E.R., 1975, *The locomotion of soft-bodied animals*, London: Edward Arnold.
11. Trueman, E.R., A.R. Brand, and P. Davis, 1966, *The Dynamics of Burrowing of Some Common Littoral Bivalves.* J Exp Biol, **44**(3): p. 469-492.
12. Energizer. *Energizer E91 AA Battery Product Datasheet*. 2009, http://data.energizer.com/PDFs/E91.pdf.
13. Hinz, E.R., 1986, *The complete book of anchoring and mooring*. 1 ed., Centreville, Md: Cornell Maritime Press.
14. McCormick, M.E., 1979, *Anchoring systems*. 1 ed., New York: Pergamon Press.
15. Chance, A.B., 2006, *Design Methodology: Chance Helical Anchor/Pile Bearing Capacity*, Hubbell Power Systems.
16. Lambe, T.W. and R.V. Whitman, 1969, *Soil Mechanics*, New York: John Wiley & Sons, p. 32.
17. Winter, A., 2008, *Video of burrowing Ensis*.
18. Sveen, J.K., 2004, *MatPIV*, http://www.math.uio.no/~jks/matpiv/.
19. Winter V, A.G., 2008, *Drag reduction mechanisms employed by burrowing razor clams (Ensis directus)* in *APS DFD*, San Antonio, TX.
20. Robertson, P.K. and R.G. Campanella, 1983, *Interpretation of cone penetration tests. Part I: Sand*
Canadian Geotechnical Journal, p. 718-733.
21. Kundu, P.K. and I.M. Cohen, 2004, *Fluid Mechanics*, 3 ed., Amsterdam: Elsevier, p. 271.
22. BatteryMart.com. *12V 35 AH Sealed Lead Acid Battery Insert Terminals*, 2009, http://www.batterymart.com/p-12v-35ah-sealed-lead-acid-battery-insert-terminal.html.
23. Scuba.com. *Sherwood 80 Cubic Foot Aluminum Tank*. 2009, http://www.scuba.com/scuba-gear-200/043077-042005/Sherwood-80-Cubic-Foot-Aluminum-Tank.html.
24. Slocum, A.H., 1992, *Precision machine design*, Englewood Cliffs, N.J: Prentice Hall, p. 482.
25. Avallone, E.A. and I. T. Baumeister, 196, *Marks' Standard Handbook for Mechanical Engineers*, 10 ed., New York: McGraw-Hill, Chapt. 3, p. 23-24.
26. Coveney, D., 2008, *RoboClam Picture*, MIT News Office.
27. *LabView 8.5*. 2008, National Instruments.
28. *MATLAB Genetic Algorithm Solver,* http://www.mathworks.com/products/gads/.